Isotope Sensitive Branching and Kinetic Isotope Effects in the Reaction of Deuterated Arachidonic Acids with Human 12- and 15-Lipoxygenases[†]

Cyril Jacquot,[‡] Aaron T. Wecksler,[§] Chris M. McGinley,[‡] Erika N. Segraves,[§] Theodore R. Holman,*[,§] and Wilfred A. van der Donk*[,‡]

Department of Chemistry, University of Illinois at Urbana−Champaign, 600 South Mathews Avenue, Urbana, Illinois 61801, and Chemistry and Biochemistry Department, University of California, Santa Cruz, Santa Cruz, California 95064

Received February 22, 2008; Revised Manuscript Received May 11, 2008

ABSTRACT: Lipoxygenases (LOs) catalyze lipid peroxidation and have been implicated in a number of human diseases connected to oxidative stress and inflammation. These enzymes have also attracted considerable attention due to large kinetic isotope effects (30−80) for the rate-limiting hydrogen abstraction step with linoleic acid (LA) as substrate. Herein, we report kinetic isotope effects (KIEs) in the reactions of three human LOs (platelet 12-hLO, reticulocyte 15-hLO-1, and epithelial 15-hLO-2) with arachidonic acid (AA). Surprisingly, the observed KIEs with AA were much smaller than the previously reported values with LA. Investigation into the origins for the smaller KIEs led to the discovery of isotope sensitive branching of the reaction pathways. Product distribution analysis demonstrated an inversion in the regioselectivity of 15-hLO-1, with hydrogen abstraction from C13 being the major pathway with unlabeled AA but abstraction from C10 predominating when the methylene group at position 13 was deuterated. Smaller but clear changes in regioselectivity were also observed for 12-hLO and 15-hLO-2.

Lipoxygenases (LOs) are non-heme iron proteins that catalyze the hydrogen atom abstraction from a bisallylic position in polyunsaturated fatty acids and the subsequent addition of molecular oxygen to the resulting substrate radical to generate hydroperoxide products (*1*). Mammalian LOs catalyze key steps in the conversion of arachidonic acid (AA),[1] a C20 tetraunsaturated fatty acid (20:4, *ω*-6), to lipoxins and leukotrienes (*2*). They have been implicated in a number of pathologies including cancer (*3, 4*), atherosclerosis (*5*), and Alzheimer's disease (*6, 7*). In plants, LOs convert linoleic acid (LA), a C18 bisunsaturated fatty acid (18:2, *ω*-6), into 13-hydroperoxyoctadecadienoic acid (13-HPODE), a precursor for jasmonates and aldehydes involved in signaling, germination, and senescence (*8*). In mammals, the isozymes are named according to the position of AA that reacts with molecular oxygen (Figure 1). Several human LOs (5-, 12-, and 15-hLOs) have thus far been identified (*9*), with this study focusing on the latter two groups. Two isozymes of 15-hLO have been characterized in humans and are called 15-hLO-1 (also termed 12/15-hLO) (*10, 11*) and 15-hLO-2 (*12*). The former exhibits a product selectivity of 15-HPETE over 12-HPETE of about a 9:1 (*13*), whereas the latter exclusively forms 15-HPETE (*12, 14*).

Lipoxygenases are mononuclear non-heme iron dependent enzymes with a unique mechanism of catalysis. Most iron dependent oxidative enzymes first activate molecular oxygen by reaction with the metal in a reduced oxidation state, with subsequent oxygen transfer to the substrate. In the case of LOs, the fatty acid substrate is first activated by hydrogen atom abstraction before reaction with molecular oxygen (*15, 16*). In resting LO, the iron is in the inactive ferrous form and needs to be converted to the active ferric form by the addition of LO products to initiate the catalytic cycle. In laboratory settings, this initiation process results in lag times before activity is observed, but these can be removed by addition of a hydroperoxide activator. After binding of the substrate to activated enzyme, a proton-coupled electron transfer from the substrate to the ferric species forms a ferrous species and an intermediate radical (Figure 2) (*17, 18*), the exact structure of which is currently unknown (*19*). After stereoselective antarafacial reaction of the organic radical with molecular oxygen (*20*), the peroxyl radical intermediate oxidizes the iron back to the active ferric state and the peroxide product is released from the enzyme.

The factors governing the regiochemistry of the oxidation of arachidonic acid have received extensive attention in the past decade. In the most current picture resulting from various

[†] This work was supported by the National Institutes of Health (GM44911 to W.A.V. and GM56062 to T.R.H.) and American Heart Association predoctoral fellowships (0615604Z to C.J. and 0310006Z to C.M.M.).

* To whom correspondence should be addressed. W.A.V.: phone, 217-244-5360; fax, 217-244-8068; e-mail, vddonk@uiuc.edu. T.R.H.: phone, 831-459-5884; fax, 831-459-2935; e-mail, tholman@chemistry.ucsc.edu.

[‡] University of Illinois at Urbana−Champaign.

[§] University of California, Santa Cruz.

[1] Abbreviations: LA, linoleic acid; AA, arachidonic acid; 15-hLO-1, human reticulocyte 15-lipoxygenase-1; 15-hLO-2, human epithelial 15-lipoxygenase-2; 12-hLO, human platelet 12-lipoxygenase; sLO-1, soybean lipoxygenase-1; 13-H(P)ODE, (9*Z*,11*E*)-13-hydro(pero)xyoctadeca-9,11-dienoic acid; 5-H(P)ETE, (6*E*,8*Z*,11*Z*,14*Z*)-5-hydro(pero)-xyeicosa-6,8,11,14-tetraenoic acid; 8-H(P)ETE, (5*Z*,9*E*,11*Z*,14*Z*)-8-hydro(pero)xyeicosa-5,9,11,14-tetraenoic acid; 11-H(P)ETE, (5*Z*,8*Z*,12*E*,14*Z*)-11-hydro(pero)xyeicosa-5,8,12,14-tetraenoic acid; 12-H(P)ETE, (5*Z*,8*Z*,10*E*,14*Z*)-12-hydro(pero)xyeicosa-5,8,10,14-tetraenoic acid; 15-H(P)ETE, (5*Z*,8*Z*,11*Z*,13*E*)-15-hydro(pero)xyeicosa-5,8,11,13-tetraenoic acid; KIE, kinetic isotope effect; HEPES, 4-(2-hydroxyethyl)-1-piperazineethanesulfonic acid; SDS−PAGE, sodium dodecyl sulfate−polyacrylamide gel electrophoresis; ICP-MS, inductively coupled plasma mass spectrometry.

10.1021/bi800308q CCC: $40.75 © 2008 American Chemical Society
Published on Web 06/12/2008

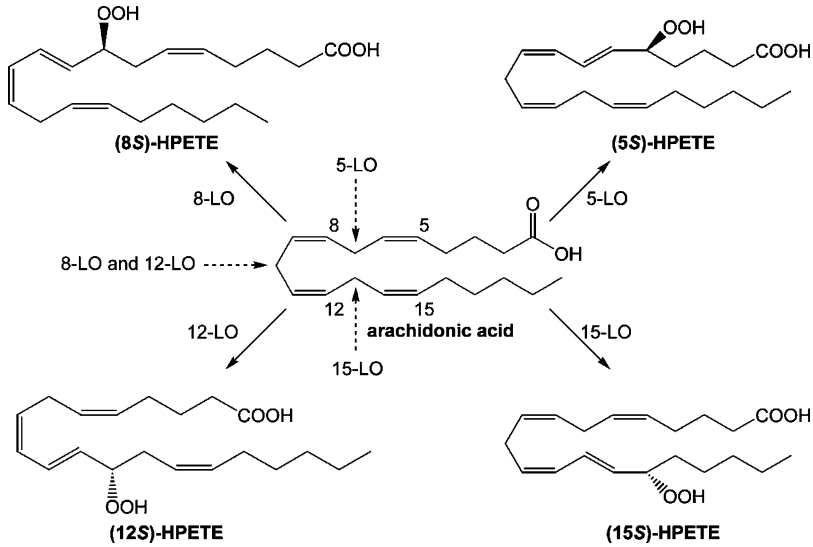

FIGURE 1: Human lipoxygenase isozymes and their respective products from oxidation of arachidonic acid. The dashed arrows indicate the position of hydrogen atom abstraction by the various enzymes. A 12*R*-LO has also been identified in humans (*1*).

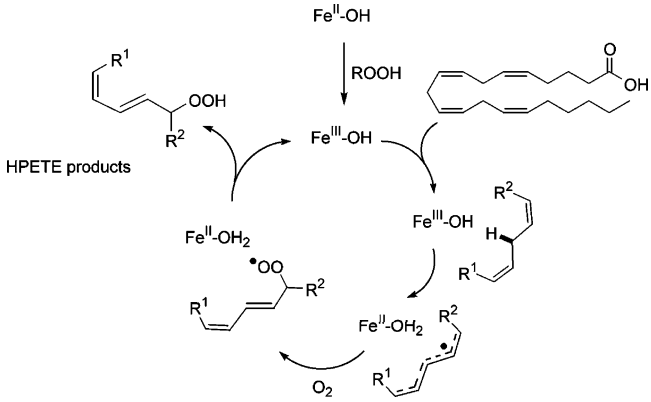

FIGURE 2: Catalytic cycle of fatty acid oxidation by lipoxygenases.

experimental approaches (*9, 20–23*), regioselective oxidation is achieved through control over the position of hydrogen atom abstraction by the geometry and size of the enzyme active site and through control by the protein over the interaction of molecular oxygen with the generated delocalized substrate radical. Several studies have reported successful changes to the regioselectivity of various lipoxygenases via site-directed mutagenesis (*9, 24*). A second aspect of lipoxygenase catalysis that has generated much interest is the unusually high kinetic isotope effects (KIEs) of 40−50 that have been observed in the hydrogen abstraction from linoleic acid by soybean lipoxygenase-1 (sLO-1) and 15-hLO-1 (*25–30*). In this study, we aimed to determine the KIEs of the reaction of human LOs with their other physiological substrate, arachidonic acid. Furthermore, we were interested whether potentially large KIEs would result in a change in regioselectivity by the smallest possible change in substrate structure, the replacement of a protium by a deuterium.

MATERIALS AND METHODS

Methods. ^{1}H NMR and ^{13}C NMR spectra were recorded on 400 and 500 MHz Varian spectrometers (100.6 and 125.6 MHz for ^{13}C) in the VOICE laboratory at the University of Illinois, Urbana−Champaign. The HPLC product analysis was performed on a reverse-phase system using a Varian Dynamax Microsorb 100-5 C18 column (25 cm × 4.6 mm) on a Rainin system (Dynamax model SD-200 pump and model UV-1 detector). 5-HETE, 8-HETE, 11-HETE, 12-HETE, 15-HETE, and 13-HODE authentic standards were purchased from Cayman Chemical Co. (Ann Arbor, MI).

Fatty Acid Synthesis. AA and LA were purchased from Sigma-Aldrich (Milwaukee, WI). 10,10-Dideuterated arachidonic acid (10-d_2-AA) and 13,13-dideuterated AA (13-d_2-AA) were synthesized as described previously (*31*). 10,10,13,13-Tetradeuterated AA (10,13-d_4-AA) was synthesized as described below. All fatty acids were purified by HPLC on a Varian Dynamax Microsorb 100-5 C18 column (25 cm × 10 mm) before use in kinetic experiments. Solution A was 99.9% acetonitrile and 0.1% acetic acid, while solution B was 99.9% water and 0.1% acetic acid. An isocratic elution of 75% A/25% B afforded purified fatty acids. The run was monitored at 210 nm and the elution time was 22 min for LA and 25 min for AA and its deuterated analogues. The fatty acids were stored at −80 °C in ethanol or benzene under argon.

Synthesis of 10,10,13,13-d_4-AA. All reactions were performed in oven-dried or flame-dried glassware under an inert atmosphere of dry nitrogen. Tetrahydrofuran was distilled from Na metal and benzophenone. Dichloromethane was distilled from CaH_2. Commercial reagents were reagent grade or better and were used as received without further purification. Analytical thin-layer chromatography was performed on Merck silica gel plates with QF-254 indicator. Visualization was performed with a $KMnO_4$ solution or a UV light. Flash column chromatography was performed using 230−400 mesh silica gel purchased from EMD Chemicals (Darmstadt, Germany). Spectra are referenced to chloroform-d_1 as an internal standard (δ 7.26 ppm, ^{1}H; δ 77.0 ppm, ^{13}C). Chemical shifts are reported in ppm (δ), and peak multiplicities are labeled as s (singlet), d (doublet), t (triplet), q (quartet), and m (multiplet). Coupling constants are given in hertz. Detailed description of procedures and spectroscopic characterization is reported in the Supporting Information.

Methyl glycolate (**1**) was protected by reaction with 3,4-dihydropyran (DHP) in dichloromethane with catalytic

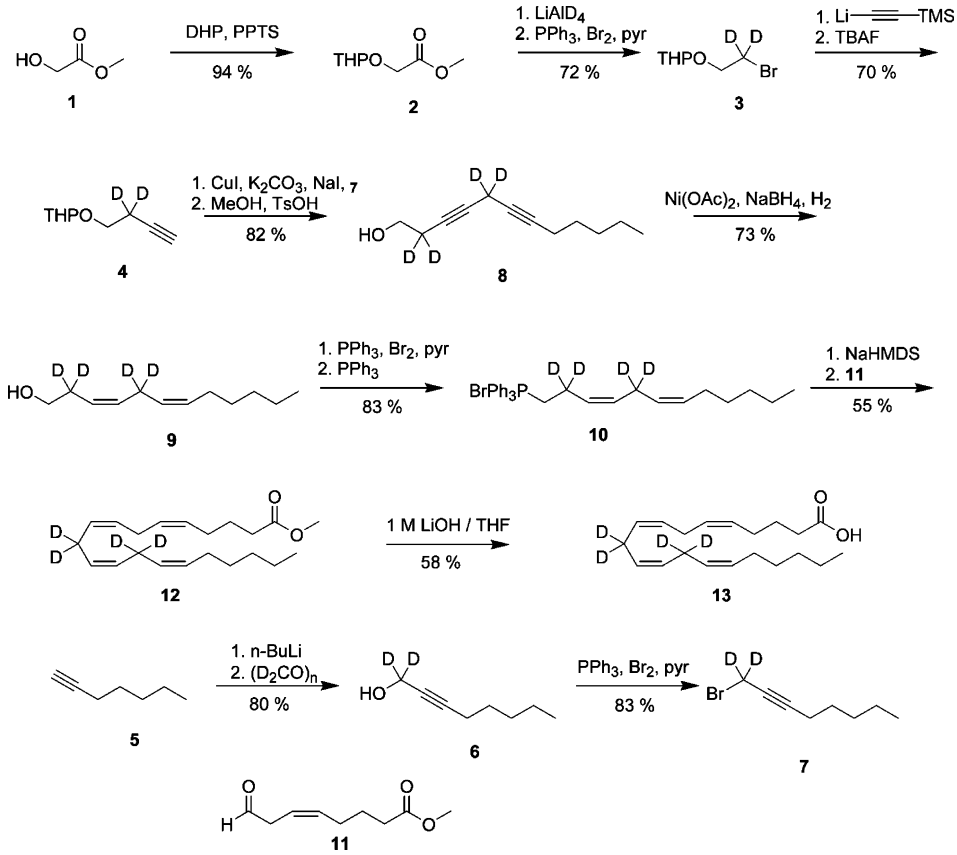

FIGURE 3: Synthetic scheme for the preparation of 10,13-d_4-AA.

pyridinium *p*-toluenesulfonate (PPTS) to provide the THP-protected alcohol. Reduction of the methyl ester **2** with lithium aluminum deuteride (98% atom D) in tetrahydrofuran (*31*) followed by bromination in dichloromethane yielded deuterated bromide **3** in good yield and isotopic purity (>95%). Reaction of intermediate **3** with a solution of lithium trimethylsilylacetylide in a mixture of tetrahydrofuran and hexamethyl phosphoramide, followed by deprotection with TBAF in tetrahydrofuran, afforded alkyne **4**. The skipped diyne **8** was formed via a copper mediated coupling of the terminal alkyne **4** with propargylic bromide **7** in dimethylformamide (*32*). The bromide coupling partner **7** was synthesized in good yield by reaction of 1-heptyne (**5**) and deuterated paraformaldehyde in tetrahydrofuran (*33*), followed by bromination of the propargylic alcohol **6** using triphenylphosphine, bromine, and pyridine in dichloromethane. Deprotection of the skipped diyne to produce **8** was accomplished using 1% toluenesulfonic acid (TsOH) in methanol. Hydrogenation mediated by nickel acetate in ethanol provided mainly the desired skipped diene **9** (*34*), with some underreduced products also observed. However, chromatographic purification using silica gel impregnated with 6% silver nitrate and elution with 45% ether/pentane yielded only the desired product in good overall yield. Then the alcohol was brominated in dichloromethane and converted to the phosphonium salt **10** in acetonitrile. A Wittig reaction between **10** and β,γ-unsaturated aldehyde **11** in tetrahydrofuran afforded the substituted methyl arachidonate **12**. Finally, basic hydrolysis with aqueous lithium hydroxide yielded the (10,10,13,13-$^2H_4$)arachidonic acid **13**. ^{1}H NMR (400 MHz, $CDCl_3$) δ 0.88 (t, J = 6.9 Hz, 3 H), 1.22−1.40 (m, 6 H), 1.72 (pentet, J = 7.4 Hz, 2 H), 2.05 (qd, J = 7.1, 1.2 Hz, 2 H), 2.07 (q, J = 7.1 Hz, 2 H), 2.36 (t, J = 7.5 Hz, 2 H), 2.78−2.83 (m, 2 H), 5.30−5.45 (m, 8 H). ^{13}C NMR (100.6 MHz, $CDCl_3$) δ 14.3 (CH_3), 22.8 (CH_2), 24.7 (CH_2), 25.8 (CH_2), 26.7 (CH_2), 27.4 (CH_2), 29.6 (CH_2), 31.7 (CH_2), 33.4 (CH_2), 127.7 (CH), 128.0 (CH), 128.4 (CH), 128.7 (CH), 129.0 (CH), 129.3 (CH), 130.8 (CH), 179.1 (Cq). Nondeuterated/partially deuterated products were not detected (limit of detection 1%). HRMS (EI, M^+) for $C_{20}H_{28}{}^2H_4O_2$ calculated 308.2654, found 308.2647.

Expression and Purification of Lipoxygenases. Platelet 12-hLO and reticulocyte 15-hLO-1 were expressed and purified as described previously (*35*). Briefly, these two enzymes contained hexa-His tags and were purified in one step by Ni^{2+} affinity chromatography. Epithelial 15-hLO-2 did not contain a His tag and was purified as previously reported with ion exchange chromatography (*36*). All enzymes were frozen at −80 °C, with glycerol added (20% for 12-hLO and 10% for 15-hLO-1 and 15-hLO-2) to prevent inactivation. The iron content of all lipoxygenase enzymes was determined on a Finnegan inductively coupled plasma mass spectrometer (ICP-MS), using internal standards of cobalt(II)-EDTA, and the data were compared with those of standardized iron solutions. All kinetic measurements were standardized to iron content. Soybean lipoxygenase-1 (sLO-1) was expressed and purified as previously described (*37*).

Steady State Kinetic Measurements of 15-hLO-1. Kinetic experiments were performed on a Cary 100 Bio UV−visible spectrophotometer. All assays were carried out in 1 mL of oxygen-saturated 25 mM HEPES buffer (pH 7.5, 25 °C) with substrate concentrations ranging from 1 to 15 μM. Enzymatic reactions were initiated by the addition of 20 nM 15-hLO-1 (normalized to iron content). Initial rates (<15% conversion)

were determined by monitoring the formation of the conjugated product (HPETE) at 235 nm ($\epsilon = 2.7 \times 10^4$ M^{-1} cm^{-1}) (*38*). No photodegradation of the product was observed at this wavelength. AA solutions were stored in absolute ethanol and diluted into buffer so that the total ethanol concentration in the kinetic assays was less than 1.5%. Fatty acid concentrations were determined by incubating the fatty acid with commercial sLO-1 (Sigma-Aldrich Chemical Co., Milwaukee, WI) and quantitating product formation at 235 nm. In order to eliminate a lag phase and obtain initial rates of the human enzymes before autoinactivation occurred, the enzymes were preactivated with 13-HPODE (*39, 40*). A solution of 13-HPODE ($\epsilon = 2.3 \times 10^4$ M^{-1} cm^{-1} at 235 nm) (*41*) was prepared by mixing linoleic acid (220 μM) and purified sLO-1 (0.5 nM) in HEPES buffer (1 mL) for 60 min at 0 °C and then filtering through a YM-30 centricon microconcentrator (Millipore, Billerica, MA) to remove any remaining sLO-1. The absence of any remaining LA from the 13-HPODE solution was verified by addition of more, fresh sLO-1. 13-HPODE was added to a final concentration of 8 μM to each kinetic assay. Initial rates for each substrate were fit to the Michaelis−Menten equation using graphing options available in KaleidaGraph (Synergy.com software).

HPLC Separation of Standards. Using an isocratic elution of 55% A/45% B afforded the separation of commercially obtained standards of 13-HODE, 15-HETE, 11-HETE, 8-HETE, 12-HETE, and 5-HETE. Under all the conditions tested, 8- and 12-HETE coeluted. The elution times were 35, 40, 45, 50, and 55 min, respectively, for 13-HODE, 15-HETE, 11-HETE, 8-HETE/12-HETE, and 5-HETE. 13-HODE is the reduction product of 13-HPODE. Note that since the analysis was not performed with a column containing a chiral stationary phase, no information was obtained regarding the stereochemistry of the enzymatic products.

HPLC Analysis of Enzymatic Products. For each 12-hLO and 15-hLO-1 run, substrate (AA, 10-d_2-AA, 13-d_2-AA or 10,13-d_4-AA; 15 μM) was combined with enzyme (12-hLO or 15-hLO-1; 50 nM) in 1 mL of HEPES buffer (25 mM, pH 7.5, 25 °C). For 15-hLO-2, the analysis was performed with AA (15 μM) and 13-d_2-AA (10 μM) by combining with 150 nM enzyme for protiated substrate and 1.8 mM enzyme for 13-d_2-AA. The reaction was monitored at 235 nm, and reaction products were isolated after 15 min for 12-hLO and 15-hLO-1, after 20 min for 15-hLO-2 and AA, and after 30 min for 15-hLO-2 and 13-d_2-AA. When the reaction stopped with 15-hLO-1, the substrate was not always entirely consumed due to enzyme autoinactivation as previously reported (*31*). However, since HPLC analysis was performed at 235 nm, unreacted AA was not visible at this wavelength and did not interfere with product analysis. The other two enzymes, 12-hLO and 15-hLO-2, completely consumed all AA in these assays. In general, three 1 mL assays were performed; the products were pooled, acidified to pH 1 using 1 N HCl (aq), and extracted with dichloromethane (5 × 2 mL). The combined organic layers were dried by passing through a Pasteur pipet containing $MgSO_4$ and concentrated under a stream of nitrogen gas.

The HPETE residues were reconstituted in dry tetrahydrofuran (120 μL) and reduced to the corresponding HETEs, because unlike HPETEs, authentic HETE standards are commercially available. An aliquot of HPETE solution (20 μL) was treated with a 0.1 M $NaBH_4$ solution in dry tetrahydrofuran (10 μL), and the reaction was allowed to proceed for 5 min at 0 °C. The reaction was quenched by adding 1 N HCl (aq) (10 μL) until gas evolution ceased. The solution was analyzed by HPLC and monitored at 235 nm as described above.

LC/MS/MS Analysis of Enzymatic Products. LC/MS/MS was performed at the Roy J. Carver Metabolomics Center at the University of Illinois, Urbana−Champaign, on an Agilent 1100 series LC system (Santa Clara, CA) using a reverse-phase Varian Dynamax Microsorb 100-5 C18 column (25 cm × 4.6 mm). Negative-mode mass spectra were acquired using an Agilent MSD Trap XCT Plus mass spectrometer equipped with an ESI source. Nitrogen was used as nebulizer gas (35 psi) and drying gas (8 L/min). The capillary voltage was set to 4.5 kV. The heated capillary of ESI source was kept at 350 °C during the analysis. Full-scan analysis was performed from *m*/*z* 55 to 350. Software Chemstation for LC 3D System Rev B.01.03 (Agilent Technologies, Santa Clara, CA) was used for LC/MS/MS system control, data acquisition, and data analysis.

RESULTS

Expression and Purification of Lipoxygenases. The three isozymes 15-hLO-1, 15-hLO-2, and 12-hLO yielded approximately 50 mg of purified protein per liter of SF9 cell culture and were greater than 90% pure as judged by SDS−PAGE. As isolated, ICP-MS indicated that the human enzymes had the following iron content: 0.33 ± 0.02 equiv per 15-hLO-1, 0.43 ± 0.02 equiv per 15-hLO-2, and 0.28 ± 0.03 equiv per 12-hLO. All kinetic data reported herein were corrected for iron content.

Kinetic Analysis of 15-hLO-1 with AA and Deuterium Labeled AA. To complement the existing KIE data for reaction of 15-hLO-1 with linoleic acid, 13-d_2-arachidonic acid was prepared (*31*). Although the double label results in a combination of primary and secondary KIEs, we elected to prepare this compound to avoid any complications from a potential change in stereoselectivity in the hydrogen atom abstraction step as has been reported in studies on sLO-1 with (11*S*)-d_1-LA (*42*). The reaction of AA and 13-d_2-AA with 15-hLO-1 was monitored at 235 nm. 13-HPODE, the product of sLO-1 oxidation of LA, was added to the assays as initiator to eliminate the lag times observed in its absence. A typical plot for the dependence of the observed initial rates on substrate concentration is shown in Figure 4. By fitting to the Michaelis−Menten rate equation, the kinetic parameters shown in Table 1 were obtained. The apparent primary kinetic isotope effect on k_{cat} at 25 °C was 3.99 ± 0.17 when comparing AA and 13-d_2-AA. This value is much smaller than the previously reported numbers under similar conditions for the oxidation of perdeuterated LA by lipoxygenases, which include a $^{D}k_{cat}$ of 50 for sLO-1 (*25*) and 40 for 15-hLO-1 (*30*). As mentioned in the introduction, one possible mechanism resulting in lower isotope effects involves a change in regioselectivity in response to deuteration at position C13. 10,13-d_4-Arachidonic acid was synthesized as described in Materials and Methods. Initial rate assays with AA and 10,13-d_4-AA demonstrated an apparent $^{D}k_{cat}$ of 9.93 ± 0.34, markedly higher than that observed with 13-d_2-AA. On the other hand, the apparent $^{D}k_{cat}$ for 10-d_2-AA was 1.07

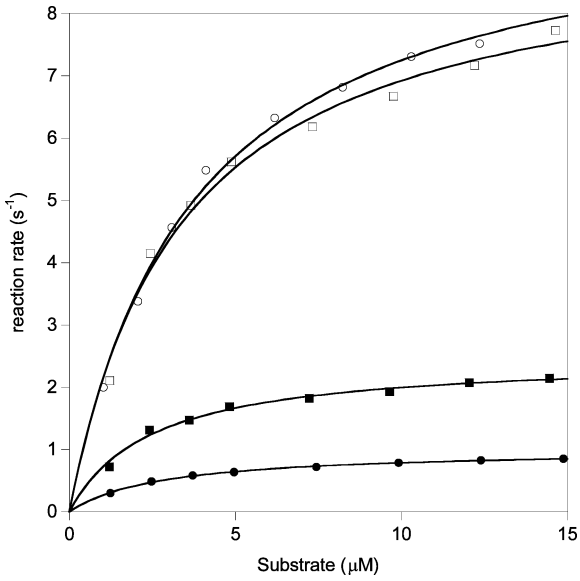

FIGURE 4: Reaction rates of the reaction of AA (open circles), 10,10-d_2-AA (open squares), 13,13-d_2-AA (filled squares), and 10,10,13,13-d_4-AA (filled circles) with 15-hLO-1 at 25 °C.

Table 1: Kinetic Parameters for the Reactions of 15-hLO-1 with Arachidonic Acids[a]

	K_M (μM)	k_{cat} (s^{-1})	apparent $^Dk_{cat}$
15-hLO-1 and AA	3.7 (0.3)	9.93 (0.28)	
15-hLO-1 and 13-d_2-AA	2.5 (0.2)	2.49 (0.08)	3.99 (0.17)
15-hLO-1 and 10-d_2-AA	3.4 (0.4)	9.26 (0.34)	1.07 (0.05)
15-hLO-1 and 10,13-d_4-AA	2.8 (0.1)	1.00 (0.04)	9.93 (0.34)

[a] Standard deviations from two independent experiments are indicated in parentheses.

$\pm$ 0.05. The observed $^Dk_{cat}$ values indicated that deuterium labeling at position C10 had little effect when position C13 was protiated, but when C13 was deuterated, the introduction of deuterium atoms on C10 had a dramatic effect on the reaction rate. These results are consistent with a change in regioselectivity, resulting in increased hydrogen abstraction from C10 when C13 is deuterated but little abstraction from C10 when C13 is protiated.

HPLC Analysis of Product Distribution. To confirm a change in regioselectivity, the product compositions of the reaction of 15-hLO-1 with arachidonic acid and its deuterated analogues were determined by HPLC after reduction of the peroxide products to the corresponding alcohols. To simplify the analysis, 13-HPODE, which had been added to the kinetic assays described above, was not added in the assays determining the product distribution. The presence or absence of 13-HPODE did not change the product distributions (Figures S1 and S2, Supporting Information). The chromatograms for the reactions of 15-hLO-1 with AA, 13-d_2-AA, and 10,13-d_4-AA are shown in Figures 5, 6, and 7, respectively. We were unable to resolve the 8- and 12-HETE products, but since both compounds originate from hydrogen atom abstraction from C10, the peak corresponding to the sum of 8-HETE and 12-HETE still provides information about the regioselectivity of the hydrogen abstraction step. Furthermore, MS/MS analysis (vide infra) on the 8/12-HETE peak produced with 15-hLO-1 showed a fragmentation pattern that was diagnostic for 12-HETE without any observed fragments indicative of 8-HETE. Similar methodology was also used to investigate the product distributions

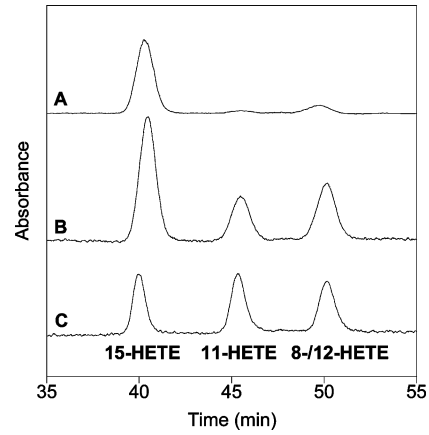

FIGURE 5: Product distribution for the reaction of 15-hLO-1 with AA. HPLC traces are shown for (A) the reduced reaction mixture and (B) the reduced reaction mixture spiked with 8-, 11-, 12-, and 15-HETE standards. Panel C displays a sample of HETE standards.

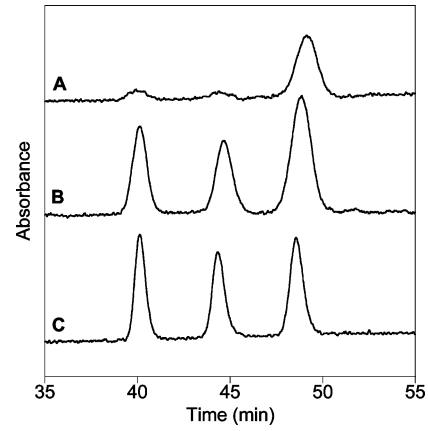

FIGURE 6: Product distribution for the reaction of 15-hLO-1 with 13-d_2-AA. HPLC traces are shown for (A) the reduced reaction mixture and (B) the reduced reaction mixture spiked with 8-, 11-, 12-, and 15-HETE standards. Panel C displays a sample of HETE standards.

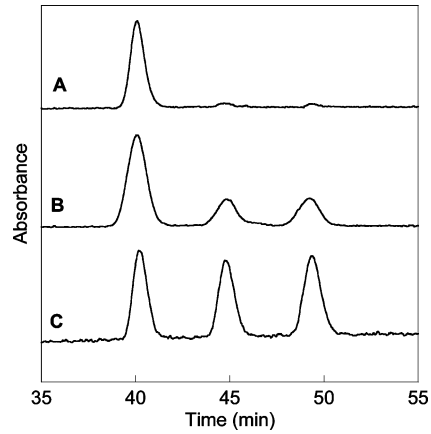

FIGURE 7: Product distribution for the reaction of 15-hLO-1 with 10,13-d_4-AA. HPLC traces are shown for (A) the reduced reaction mixture and (B) the reduced reaction mixture spiked with 8-, 11-, 12-, and 15-HETE standards. Panel C displays a sample of HETE standards.

for the reactions of 15-hLO-2 and 12-hLO (Figures S4−S9, Supporting Information). A summary of the product distributions is provided in Table 2.

As reported previously (*13*), the reaction of 15-hLO-1 with unlabeled AA generated mostly products from hydrogen

Table 2: Product Distributions of Lipoxygenases under Various Conditions[a]

entry	conditions	15-HETE (%)	11-HETE (%)	8/12-HETE (%)
1	15-hLO-1 and AA	85 (3)	4 (1)	11 (3)
2	15-hLO-1 and 13-d_2-AA	15 (1)	10 (2)	75 (2)
3	15-hLO-1 and 10-d_2-AA	93 (1)	4 (1)	3 (1)
4	15-hLO-1 and 10,13-d_4-AA	82 (2)	9 (2)	9 (2)
5	15-hLO-2 and AA	94 (1)	4 (1)	2 (1)
6	15-hLO-2 and 13-d_2-AA	82 (2)	7 (1)	11 (2)
7	12-hLO and AA	6 (2)	5 (2)	89 (4)
8	12-hLO and 10-d_2-AA	11 (3)	12 (3)	77 (2)
9	12-hLO and 13-d_2-AA	1 (1)	5 (2)	94 (2)
10	12-hLO and 10,13-d_4-AA	4 (2)	8 (2)	88 (2)

[a] Standard deviations from three independent experiments are indicated in parentheses.

abstraction from C13 (89% 11- and 15-HETE) with minor products derived from abstraction from C10 (11% 12-HETE) (entry 1, Table 2). As displayed in Figures 5A and 6A, the selectivity shifted dramatically when the enzyme was presented with 13,13-dideuterated AA with products derived from hydrogen abstraction at position C10 predominating by a 75% to 25% margin (entry 2). With 10,10-dideuterated AA as substrate, the enzyme was more selective for abstraction from the C13 position (97%, entry 3) compared to the reaction with unlabeled substrate (entry 1), whereas with tetradeuterated AA, the ratio of products was close to that with unlabeled substrate (entry 4).

15-hLO-2 has been reported previously to exclusively produce 15-HPETE (*12*), and we cannot rule out that the very small amount of other products we observed (Figure S4, Supporting Information) are impurities. With 13,13-d_2-AA as substrate, the selectivity of 15-hLO-2 remained skewed toward C13 hydrogen abstraction products (89%) compared to C10 abstraction products (11%), but the selectivity was decreased compared to unlabeled AA (entries 5 and 6, Figure S5, Supporting Information). With protiated and 10,13-tetradeuterated AA, 12-hLO formed mainly 12-HPETE over 11- and 15-HPETE (entries 7 and 10). With 10-d_2-AA, the selectivity for hydrogen abstraction from C10 decreased from 89% to 77% while products from hydrogen abstraction from C13 increased from 11% to 23% (entry 8). In the presence of 13,13-dideuterated AA, the selectivity for abstraction at C10 was slightly increased compared to using unlabeled AA (entry 9). 5-HETE was not observed under any conditions.

LC/MS/MS Analysis of Enzymatic Products. To confirm the identity of the products in the HPLC traces more rigorously, mass spectrometric analysis was performed on the reaction products formed upon incubation of 15-hLO-1 with unlabeled AA and 13-d_2-AA. These two conditions resulted in the largest change in enzyme regioselectivity. The fragmentation results for the reaction with AA are shown in Figure 8. The fragmentation patterns were compared to those obtained from HETE standards and to a previous literature report (*43*). The LC/MS/MS data confirmed the assignments of the structures of the products made in the previous section based on HPLC retention times.

A similar analysis was performed for the products of 13-d_2-AA incubated with 15-hLO-1 (Figure 9). The first eluting peak showed a mass that was diagnostic of the presence of one deuterium atom, with a fragmentation pattern consistent with 15-HETE containing one deuterium at C13. The last peak showed a mass indicating the presence of two deuterium atoms and a fragmentation pattern consistent with 12-HETE labeled at the C13 position. Unfortunately, the signal-to-noise ratio of the mass spectrum obtained of the middle peak was such that no firm conclusions regarding the identity of the material could be made. In both the reaction of 15-hLO-1 with AA and 13-d_2-AA, the fragmentation pattern of the 12-HETE peak did not show any characteristic fragments from 8-HETE, suggesting that this isomer was not formed.

DISCUSSION

Soybean and mammalian LOs exhibit extremely large kinetic isotope effects (*25–30*). These observations have led to a model in which quantum mechanical tunneling is coupled to environmental motions governed by protein dynamics (*44*). Thus far, kinetic isotope effect studies of LOs have focused on linoleic acid because deuterium labeled analogues are commercially available or can be prepared in relatively few steps. Isotope effects for oxidation of the prototypical and therapeutically important substrate arachidonic acid have not been investigated since the suitably deuterated analogues are not readily obtained. Using appropriately labeled synthetic AA substrates in this work, a KIE on k_{cat} of ~4 was observed in reactions of 15-hLO-1. The KIE increased to ~10 when the enzyme was presented with 10,13-tetradeuterated AA. The deuterium substitution at the presumably unreactive C10 position should not have affected the rate of reaction if it were proceeding exclusively via hydrogen atom abstraction from C13. Indeed, analysis of the product distribution revealed a remarkable reversal of the regioselectivity of hydrogen atom abstraction when 15-hLO-1 was presented with 13-d_2-AA.

Lipoxygenases abstract hydrogen atoms from bisallylic methylene groups with weak C−H bonds. Three such positions are present in arachidonic acid (Figure 1). C13 is the predominant site of abstraction for 15-LO resulting in a substrate radical that is presumably delocalized over the C11−C15 carbon chain, although the exact structure(s) of the radical is unknown (*20*). If it is a pentadienyl radical, as is observed in the oxidation of AA by prostaglandin H synthase (*45, 46*), or exists as a mixture of interconverting allyl radicals, two possible sites exist for oxygen attack giving 11-HPETE or 15-HPETE. On the other hand, abstraction at C10 proceeds to 8-HPETE or 12-HPETE. 15-hLO-1 normally displays a preference for C13 abstraction, but when presented with 13,13-dideuterated arachidonic acid, the isotope effect on hydrogen atom abstraction resulted in ~75% abstraction from C10. The observed outcome is an example of isotope sensitive branching, a process in which a change occurs in product distribution in response to decreasing the rate of a step at a branch point of a reaction manifold by isotopic substitution (*47*).

15-hLO-2 and 12-hLO also displayed isotope sensitive branching, but the extent to which the product distribution was changed was significantly smaller, in line with the higher regioselectivity exhibited by these proteins with unlabeled arachidonic acid. In the case of 12-hLO, the selectivity for hydrogen abstraction at C10 decreased from 89% to 77% upon deuteration at C10. Meanwhile, 15-hLO-2 showed slightly attenuated selectivity for abstraction from C13 (98%

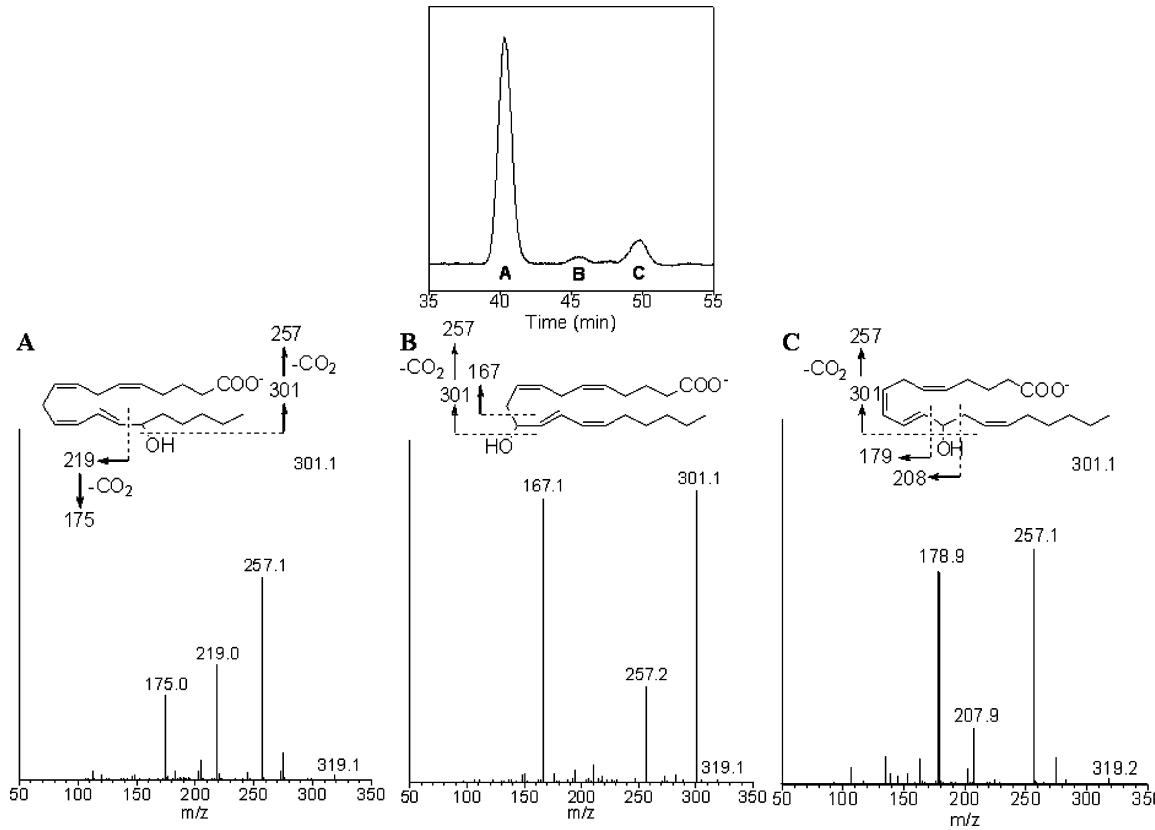

FIGURE 8: Mass fragmentation data on the products of the reaction of 15-hLO-1 with unlabeled AA. Comparison with spectra obtained from HETE standards indicates that peak A corresponds to 15-HETE, peak B to 11-HETE, and peak C to 12-HETE.

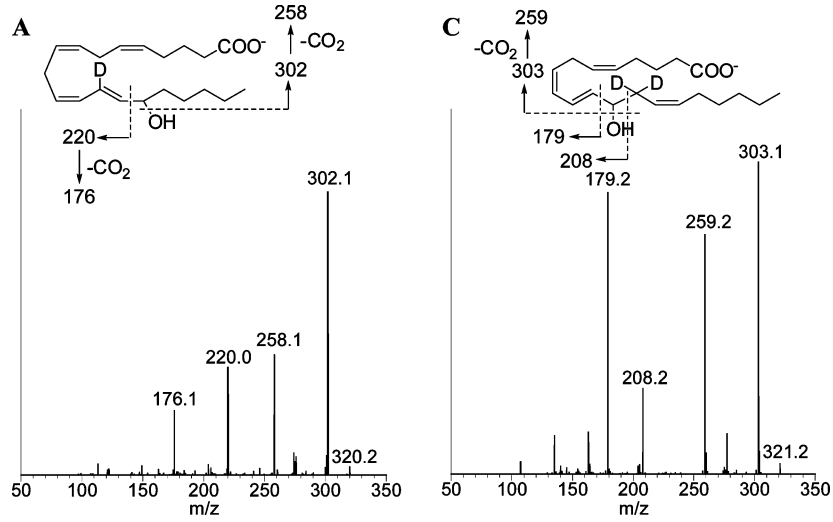

FIGURE 9: Mass fragmentation data on the products of incubation of 15-hLO-1 with 13,13-d_2-AA. The spectra show that peak A corresponds to 13-d_1-15-HETE and peak C to 13,13-d_2-12-HETE.

to 89%) when presented with 13-d_2-AA. Products arising from abstraction from C7 were not detected in any of the experiments. These findings are consistent with previous observations that converting a 15-hLO to a 12-hLO can be achieved relatively readily by mutagenesis (*9, 24*), whereas conversion of a 5-LO into a 12- or 15-LO or vice versa is significantly more challenging (*9*). The factors that govern the regioselectivity of hydrogen atom abstraction in lipoxygenases have been extensively studied using alternative substrates, site-directed mutants, different assay conditions, and X-ray crystallography (*9, 20–23, 48*). To the best of our knowledge, this study provides the first example of a change in regioselectivity based on a sterically conservative isotopic substitution. The different sensitivity of the three hLOs to isotope sensitive branching reflects both the inherently different regioselectivities with unlabeled arachidonic acids and possible differences in the size of the isotope effects on hydrogen atom abstraction. Experiments are in progress to determine the isotope effects for 12-hLO and 15-hLO-2, but these studies are beyond the scope of this work.

Assuming that the hydrogen atom abstraction step is rate limiting for k_{cat}, as is observed in other studies on LOs (*27, 30*), the observed rates in Table 1 can be used in conjunction with the product distribution in Table 2 to deconvolute the relative rates for hydrogen and deuterium atom abstraction steps from C10 and C13. The observed rate and product

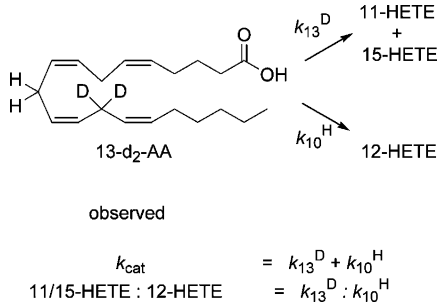

FIGURE 10: Illustration of the use of kinetic data (k_{cat}) and product distribution (11/15-HETE:8/12-HETE) to determine the rates for hydrogen and deuterium atom abstraction from C10 and C13. In this example the two experimentally determined pieces of data are used to obtain the rates of hydrogen abstraction from C10 and deuterium abstraction from C13.

Table 3: Relative Rates for Hydrogen Abstraction from Positions C10 and C13 by Human 15-Lipoxygenase-1 and Various Arachidonic Acid Analogues[a]

conditions	k_{C13} (s^{-1})	k_{C10} (s^{-1})
15-hLO-1 and AA	$k_{13}^{H} = 8.8$ (0.3)	$k_{10}^{H} = 1.10$ (0.10)
15-hLO-1 and 10-d_2-AA	$k_{13}^{H} = 9.0$ (0.3)	$k_{10}^{D} = 0.26$ (0.01)
15-hLO-1 and 13-d_2-AA	$k_{13}^{D} = 0.62$ (0.08)	$k_{10}^{H} = 1.87$ (0.15)
15-hLO-1 and 10,13-d_4-AA	$k_{13}^{D} = 0.91$ (0.08)	$k_{10}^{D} = 0.09$ (0.01)

[a] Error bars are indicated in parentheses.

distribution provides for each substrate two equations with two unknowns that can be solved. For example, for the reaction of 15-hLO-1 with 13-d_2-AA, the rates for *hydrogen* abstraction from C10 and *deuterium* abstraction from C13 can be determined by the observed product distribution and the observed k_{cat} (Figure 10). Similarly, the rates of *hydrogen* abstraction from C13 and *deuterium* abstraction from C10 can be determined from the data obtained with 10-d_2-AA, and the rates of hydrogen atom abstraction from C10 and C13 can be deduced from the observed rates and products with unlabeled AA. Finally, the rates of deuterium abstraction from C10 and C13 are provided by the data with 10,13-d_4-AA. The rates so obtained from different sets of experiments show good to excellent internal consistency (Table 3). Taking the averages of the derived rate constants in Table 3 suggests that the true $^{D}k_{cat}$ is 11.6 ± 2.0 for abstraction from C13 and 8.5 ± 4.0 for abstraction from C10. In classical terms, it suggests that the transition states for hydrogen atom abstraction from C10 and C13 are very similar. The much smaller KIEs observed in this work with AA also raise the question whether the hydrogen atom transfer/PCET step involves quantum mechanical tunneling. Investigations of the temperature dependence of the isotope effects to address this question are currently underway. Because of the larger relative errors on the product distribution data obtained for 12-hLO and 15-hLO-2, a similar treatment for these enzymes was not meaningful.

In summary, we synthesized a number of deuterium substituted arachidonic acids and measured their rates of reaction with three human lipoxygenases. The product distribution demonstrates that the regioselectivity of the enzymes changes when the enzymes are presented with deuterated compounds. Whereas 12-hLO and 15-hLO-2 maintained high regioselectivity for the product formed with unlabeled arachidonic acid substrate, 15-hLO-1 displayed a reversal of selectivity to bypass abstracting a deuterium atom. When adjusted for the observed isotope sensitive branching, the kinetic isotope effect on k_{cat} for hydrogen atom abstraction from C13 of AA by 15-hLO-1 was much smaller than that previously reported for the reaction of lipoxygenases with linoleic acid. Interestingly, $^{D}k_{cat}$ for abstraction from C10 and C13 were quite similar, suggesting similar transition state structures.

ACKNOWLEDGMENT

We thank Dr. Lucas Li for assistance with the LC/MS/MS analysis of HETE samples.

SUPPORTING INFORMATION AVAILABLE

Synthetic procedures for 10,10,13,13-d_4-arachidonic acid and HPLC traces displaying product distributions of the human lipoxygenase reactions. This material is available free of charge via the Internet at http://pubs.acs.org.

REFERENCES

1. Brash, A. R. (1999) Lipoxygenases: occurrence, functions, catalysis, and acquisition of substrate. *J. Biol. Chem. 274*, 23679–23682.
2. Funk, C. D. (2005) Leukotriene modifiers as potential therapeutics for cardiovascular disease. *Nat. Rev. Drug Disc. 4*, 664–672.
3. Connolly, J. M., and Rose, D. P. (1998) Enhanced angiogenesis and growth of 12-lipoxygenase gene-transfected MCF-7 human breast cancer cells in athymic nude mice. *Cancer Lett. 132*, 107–112.
4. Kamitani, H., Geller, M., and Eling, T. (1998) Expression of 15-lipoxygenase by human colorectal carcinoma Caco-2 cells during apoptosis and cell differentiation. *J. Biol. Chem. 273*, 21569–21577.
5. Harats, D., Shaish, A., George, J., Mulkins, M., Kurihara, H., Levkovitz, H., and Sigal, E. (2000) Overexpression of 15-lipoxygenase in vascular endothelium accelerates early atherosclerosis in LDL receptor-deficient mice. *Arterioscl., Thromb., Vasc. Biol. 20*, 2100–2105.
6. Pratico, D., Zhukareva, V., Yao, Y., Uryu, K., Funk, C. D., Lawson, J. A., Trojanowski, J. Q., and Lee, V. M. Y. (2004) 12/15-Lipoxygenase is increased in Alzheimer's disease: possible involvement in brain oxidative stress. *Am. J. Pathol. 164*, 1655–1662.
7. Yao, Y., Clark, C. M., Trojanowski, J. Q., Lee, V. M. Y., and Pratico, D. (2005) Elevation of 12/15-lipoxygenase products in AD and mild cognitive impairment. *Ann. Neurol. 58*, 623–626.
8. Gardner, H. W. (1991) Recent investigations into the lipoxygenase pathway of plants. *Biochim. Biophys. Acta 1084*, 221–239.
9. Kuhn, H. (2000) Structural basis for the positional specificity of lipoxygenases. *Prostaglandins Other Lipid Mediat. 62*, 255–270.
10. Sigal, E., Grunberger, D., Craik, C. S., Caughey, G. H., and Nadel, J. A. (1988) Arachidonate 15-lipoxygenase (omega-6 lipoxygenase) from human leukocytes. Purification and structural homology to other mammalian lipoxygenases. *J. Biol. Chem. 263*, 5328–5332.
11. Sigal, E., Craik, C. S., Highland, E., Grunberger, D., Costello, L. L., Dixon, R. A. F., and Nadel, J. A. (1988) Molecular cloning and primary structure of human 15-lipoxygenase. *Biochem. Biophys. Res. Commun. 157*, 457–464.
12. Brash, A. R., Boeglin, W. E., and Chang, M. S. (1997) Discovery of a second 15S-lipoxygenase in humans. *Proc. Natl. Acad. Sci. U.S.A. 94*, 6148–6152.
13. Gan, Q. F., Browner, M. F., Sloane, D. L., and Sigal, E. (1996) Defining the arachidonic acid binding site of human 15-lipoxygenase. Molecular modeling and mutagenesis. *J. Biol. Chem. 271*, 25412–25418.
14. Kilty, I., Logan, A., and Vickers, P. J. (1999) Differential characteristics of human 15-lipoxygenase isozymes and a novel splice variant of 15S-lipoxygenase. *Eur. J. Biochem. 266*, 83–93.
15. Glickman, M. H., and Klinman, J. P. (1996) Lipoxygenase reaction mechanism: demonstration that hydrogen abstraction from substrate precedes dioxygen binding during catalytic turnover. *Biochemistry 35*, 12882–12892.
16. McGinley, C. M., and van der Donk, W. A. (2003) Enzymatic hydrogen atom abstraction from polyunsaturated fatty acids. *Chem. Commun.* 2843–2846.

17. Hatcher, E., Soudackov, A. V., and Hammes-Schiffer, S. (2004) Proton-coupled electron transfer in soybean lipoxygenase. *J. Am. Chem. Soc. 126*, 5763–5775.
18. Lehnert, N., and Solomon, E. I. (2003) Density-functional investigation on the mechanism of H-atom abstraction by lipoxygenase. *J. Biol. Inorg. Chem. 8*, 294–305.
19. Nelson, M. J., Cowling, R. A., and Seitz, S. P. (1994) Structural characterization of alkyl and peroxyl radicals in solutions of purple lipoxygenase. *Biochemistry 33*, 4966–4973.
20. Schneider, C., Pratt, D. A., Porter, N. A., and Brash, A. R. (2007) Control of oxygenation in lipoxygenase and cyclooxygenase catalysis. *Chem. Biol. 14*, 473–488.
21. Gillmor, S. A., Villasenor, A., Fletterick, R., Sigal, E., and Browner, M. F. (1997) The structure of mammalian 15-lipoxygenase reveals similarity to the lipases and the determinants of substrate specificity. *Nat. Struct. Biol. 4*, 1003–1009.
22. Knapp, M. J., Seebeck, F. P., and Klinman, J. P. (2001) Steric control of oxygenation regiochemistry in soybean lipoxygenase-1. *J. Am. Chem. Soc. 123* 2931–2932.
23. Knapp, M. J., and Klinman, J. P. (2003) Kinetic studies of oxygen reactivity in soybean lipoxygenase-1. *Biochemistry 42*, 11466–11475.
24. Coffa, G., Schneider, C., and Brash, A. R. (2005) A comprehensive model of positional and stereo control in lipoxygenases. *Biochem. Biophys. Res. Commun. 338*, 87–92.
25. Glickman, M. H., Wiseman, J. S., and Klinman, J. P. (1994) Extremely large isotope effects in the soybean lipoxygenase-linoleic acid reaction. *J. Am. Chem. Soc. 116*, 793–794.
26. Hwang, C. C., and Grissom, C. B. (1994) Unusually large deuterium isotope effect in soybean lipoxygenase is not caused by a magnetic isotope effect. *J. Am. Chem. Soc. 116*, 795–796.
27. Glickman, M. H., and Klinman, J. P. (1995) Nature of rate-limiting steps in the soybean lipoxygenase-1 reaction. *Biochemistry 34*, 14077–14092.
28. Jonsson, T., Glickman, M. H., Sun, S., and Klinman, J. P. (1996) Experimental evidence for extensive tunneling of hydrogen in the lipoxygenase reaction: implications for enzyme catalysis. *J. Am. Chem. Soc. 118*, 10319–10320.
29. Lewis, E. R., Johansen, E., and Holman, T. R. (1999) Large competitive kinetic isotope effects in human 15-lipoxygenase catalysis measured by a novel HPLC method. *J. Am. Chem. Soc. 121*, 1395–1396.
30. Segraves, E. N., and Holman, T. R. (2003) Kinetic investigations of the rate-limiting step in human 12- and 15-lipoxygenase. *Biochemistry 42*, 5236–5243.
31. Peng, S., McGinley, C. M., and van der Donk, W. A. (2004) Synthesis of site-specifically labeled arachidonic acids as mechanistic probes for prostaglandin H synthase. *Org. Lett. 6*, 349–352.
32. Tallman, K. A., Roschek, B., Jr., and Porter, N. A. (2004) Factors influencing the autoxidation of fatty acids: effect of olefin geometry of the nonconjugated diene. *J. Am. Chem. Soc. 126*, 9240–9247.
33. Hutzinger, M. W., and Oehlschlager, A. C. (1995) Stereoselective synthesis of 1,4-dienes. Application to the preparation of insect pheromones (3Z,6Z)-dodeca-3,6-dien-1-ol and (4E,7Z)-trideca-4,7-dienyl acetate. *J. Org. Chem. 60*, 4595–4601.
34. Stefani, H. A., Cardoso, L. D. G., Valduga, C. J., and Zeni, G. (2001) Study of the regioselectivity in the hydrotelluration of hydroxy alkynes. *Phosphorus, Sulfur Silicon Relat. Elem. 171−172*, 421–426.
35. Amagata, T., Whitman, S., Johnson, T. A., Stessman, C. C., Loo, C. P., Lobkovsky, E., Clardy, J., Crews, P., and Holman, T. R. (2003) Exploring sponge-derived terpenoids for their potency and selectivity against 12-human, 15-human, and 15-soybean lipoxygenases. *J. Nat. Prod. 66*, 230–235.
36. Deschamps, J. D., Gautschi, J. T., Whitman, S., Johnson, T. A., Gassner, N. C., Crews, P., and Holman, T. R. (2007) Discovery of platelet-type 12-human lipoxygenase selective inhibitors by high-throughput screening of structurally diverse libraries. *Bioorg. Med. Chem. 15*, 6900–6908.
37. Holman, T. R., Zhou, J., and Solomon, E. I. (1998) Spectroscopic and functional characterization of a ligand coordination mutant of soybean lipoxygenase-1: first coordination sphere analog of human 15-lipoxygenase. *J. Am. Chem. Soc. 120*, 12564–12572.
38. Guajardo, M. H., Terrasa, A. M., and Catala, A. (2002) Retinal fatty acid binding protein reduce lipid peroxidation stimulated by long-chain fatty acid hydroperoxides on rod outer segments. *Biochim. Biophys. Acta 1581*, 65–74.
39. Schilstra, M. J., Veldink, G. A., Verhagen, J., and Vliegenthart, J. F. G. (1992) Effect of lipid hydroperoxide on lipoxygenase kinetics. *Biochemistry 31*, 7692–7699.
40. Schilstra, M. J., Veldink, G. A., and Vliegenthart, J. F. G. (1994) The dioxygenation rate in lipoxygenase catalysis is determined by the amount of iron(III) lipoxygenase in solution. *Biochemistry 33*, 3974–3979.
41. Gibian, M. J., and Vandenberg, P. (1987) Product yield in oxygenation of linoleate by soybean lipoxygenase: the value of the molar extinction coefficient in the spectrophotometric assay. *Anal. Biochem. 163*, 343–349.
42. Rickert, K. W., and Klinman, J. P. (1999) Nature of hydrogen transfer in soybean lipoxygenase-1: separation of primary and secondary isotope effects. *Biochemistry 38*, 12218–12228.
43. Murphy, R. C., Barkley, R. M., Zemski Berry, K., Hankin, J., Harrison, K., Johnson, C., Krank, J., McAnoy, A., Uhlson, C., and Zarini, S. (2005) Electrospray ionization and tandem mass spectrometry of eicosanoids. *Anal. Biochem. 346*, 1–42.
44. Knapp, M. J., and Klinman, J. P. (2002) Environmentally coupled hydrogen tunneling. Linking catalysis to dynamics. *Eur. J. Biochem. 269*, 3113–3121.
45. Peng, S., Okeley, N. M., Tsai, A.-L., Wu, G., Kulmacz, R. J., and van der Donk, W. A. (2001) Structural characterization of a pentadienyl radical intermediate formed during catalysis by prostaglandin H synthase-2. *J. Am. Chem. Soc. 123*, 3609–3610.
46. Peng, S., Okeley, N. M., Tsai, A.-L., Wu, G., Kulmacz, R. J., and van der Donk, W. A. (2002) Synthesis of isotopically labeled arachidonic acids to probe the reaction mechanism of prostaglandin H synthase. *J. Am. Chem. Soc. 124*, 10785–10796.
47. Jones, J. P., Korzekwa, K. R., Rettie, A. E., and Trager, W. F. (1986) Isotopically sensitive branching and its effect on the observed intramolecular isotope effects in cytochrome P-450 catalyzed reactions: a new method for the estimation of intrinsic isotope effects. *J. Am. Chem. Soc. 108*, 7074–7078.
48. Saam, J., Ivanov, I., Walther, M., Holzhuetter, H.-G., and Kuehn, H. (2007) Molecular dioxygen enters the active site of 12/15-lipoxygenase via dynamic oxygen access channels. *Proc. Natl. Acad. Sci. U.S.A. 104*, 13319–13324.

BI800308Q